



HAL
open science

The IAU recommended photometric system for ultraviolet astronomy

Ana Gómez de Castro, Noah Brosch, Daniela Bettoni, Leire Beitia-Antero,
Paul Scowen, David Valls-Gabaud, Mikhail Sachkov

► **To cite this version:**

Ana Gómez de Castro, Noah Brosch, Daniela Bettoni, Leire Beitia-Antero, Paul Scowen, et al.. The IAU recommended photometric system for ultraviolet astronomy. *Experimental Astronomy*, 2023, 56 (1), pp.171-195. 10.1007/s10686-023-09894-9 . hal-04310139

HAL Id: hal-04310139

<https://cnrs.hal.science/hal-04310139v1>

Submitted on 1 Dec 2023

HAL is a multi-disciplinary open access archive for the deposit and dissemination of scientific research documents, whether they are published or not. The documents may come from teaching and research institutions in France or abroad, or from public or private research centers.

L'archive ouverte pluridisciplinaire **HAL**, est destinée au dépôt et à la diffusion de documents scientifiques de niveau recherche, publiés ou non, émanant des établissements d'enseignement et de recherche français ou étrangers, des laboratoires publics ou privés.



Distributed under a Creative Commons Attribution 4.0 International License



The IAU recommended photometric system for ultraviolet astronomy

Ana I. Gómez de Castro^{1,2} · Noah Brosch³ · Daniela Bettoni⁴ ·
Leire Beitia-Antero^{1,5} · Paul Scowen⁶ · David Valls-Gabaud⁷ ·
Mikhail Sachkov⁸

Received: 30 August 2022 / Accepted: 15 March 2023 / Published online: 24 June 2023
© The Author(s) 2023

Abstract

In the current era when access to space is becoming easier and at a lower cost thanks to the standardised cubesat technology, numerous missions are expected to be launched to observe, particularly, at ultraviolet wavelengths. Given the reduced dimensions of the telescope that a cubesat can carry, most of these missions will be focused on photometric surveys of a reduced sample of targets of interest, and therefore each mission will define their own photometric bands according to their scientific objectives and orbital constraints. However, in order to provide a coherent view of the ultraviolet sky, the data should be post-processed under a common framework. In 2017, the IAU working group on ultraviolet astronomy identified the need to define such a common framework for the upcoming ultraviolet missions, and coordinated the definition of a standard set of photometric bands that could serve for homogenizing the current and future data. This paper presents the procedure adopted by the working group for the definition of the standard photometric system, that was approved by the IAU during the General Assembly Business Sessions held in August, 2021. The photometric system consists of seven bands, denoted as UV1-UV7, all included in the range 115 - 400 nm. Some of these bands are based on existing filters, while others have been defined as theoretical bands with constant throughput. This system is to be regarded as a set of synthetic bands for post-processing the data of any mission, and an example of its application to the SPARCS cubesat is also included. The photometric bands are publicly available and can be downloaded from <https://www.nuva.eu/uv-photometry/>.

Keywords Ultraviolet: general · Techniques: photometric · Instrumentation: detectors · Methods: observational · Ultraviolet: ISM

✉ Ana I. Gómez de Castro
aig@ucm.es

Extended author information available on the last page of the article

1 Introduction

Ultraviolet (UV) astronomy was born in the late sixties with the advent of space astronomy. Ever since, a well defined set of photometric standards has been carried over from mission to mission ensuring the accuracy and consistency of the data.

This *controlled* approach is going to change during the next decade with the advent of widespread use of cubesat technology. Access to UV data is fundamental in many areas of astrophysical research, however no pure UV observatories are included in the strategic planning of the main space agencies with the only exception of the Spektr-UV (WSO-UV, [39]) observatory from the Russian space science program, and the more distant NASA Habitable Worlds Observatory projected to fly in the 2040s. ULTRASAT [6] will be launched around 2025, and a MIDEX-class mission, UVEX, has been funded for a phase-A study [31]. Several other missions are under study, such as CASTOR [15] MESSIER [49], UV-SCOPE [2], HYPERION [26], and ASPERA [14], among others. CubeSats such as CUTE [21] have also been launched and it is expected that many SmallSat- and CubeSat-scale missions will be flown to run well-defined experiments, including survey-type probes [see [23], for a recent compilation of the operational UV missions, those under construction and their main goals].

In this context, it is necessary to define some common foundations to facilitate comparing and contrasting data from different UV missions. From 2018 till 2021, the charter of the UV astronomy working group (UVA WG) of the International Astronomical Union (IAU) was to set the foundations for the definition of such standards: a UV photometric system suitable to be implemented from large to small missions and that grows with the scientific challenges addressed by using UV astronomical instrumentation.

The recommendations made by the UVA WG were backed at the IAU General Assembly (Resolution B4¹) and approved with the strong support of the community. This article summarizes the contents of the report elaborated by the UVA WG during their study, as well as the description of the recommended photometric system itself. In Section 2, the contents of the astronomical databases in terms of photometric data at UV wavelengths are reviewed. The key technologies involved in shaping the UV bands are described in Section 3. The actual photometric system recommended by the IAU is described in Section 4 and the procedures for its implementation in Section 5. A short discussion on the main advantages and limitations of the system is included in Section 6. The procedures followed by the UVA WG to raise the opinion of the community are briefly summarized in [Appendix](#) for the historical record.

2 UV photometry from already-flown missions

The history of UV astronomy begins with small instruments deployed on the early space probes such as the Carruther's lunar telescope [13]. The first purpose-built astronomical observatory was launched in 1972 by NASA: the Copernicus (OAO-3,

¹ <https://www.iau.org/news/pressreleases/detail/iau2106/>

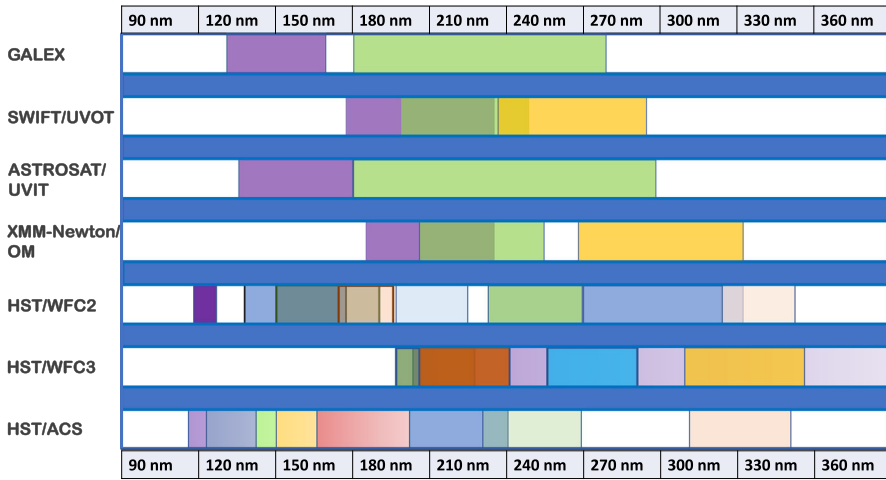


Fig. 1 Sketch outlining the spectral coverage of the UV filters (or bands) used for imaging purposes in astronomy (GALEX, Astrosat/UVIT, HST/ACS, HST/STIS, XMM-Newton/OM, SWIFT/UVOT). Note that the actual effective passbands also depend on the response of the detector. This is particularly relevant for the MCP type detectors, often used in UV Astronomy, since they use photocathodes only sensitive to specific spectral ranges. We refer the reader to the Instrument manuals and handbooks for more details on the filters (precise transmittance curves, effective wavelengths, etc.) in each case. Note that, for instance, several ACS filters are step filters that cannot be adequately represented in this plot. Also, the HST instruments possess many filters that have a high degree of spectral overlap

[38]) mission. Copernicus was equipped with instrumentation for spectroscopy in the 90-315 nm spectral range. Subsequent missions have included the International Ultraviolet Explorer (IUE, [7]), 1978-1996, for UV spectroscopy in the 115-315 nm range, the Far UV Spectroscopic Explorer (FUSE, [36]), 1999-2007, for spectroscopy in the 90.5-119.5 nm range, the GALaxy Evolution eXplorer (GALEX, [35]), 2003-2012, for imaging and slit-less spectroscopy in the 135-280 nm range and the Hubble Space Telescope (HST) (<https://www.stsci.edu/hst/>), launched in 1990 and still operational, to observe in the 115-350 nm range both in imaging and spectroscopic modes. Also flown have been SWIFT/UVOT [22], XMM-Newton/OM [30] and Astrosat/UVIT [44] which had moderate UV photometric capabilities. In Fig. 1, the UV photometric bands (or filters) used by these missions for imaging purposes are outlined. Table 1 provides a summary, extracted from the metadata of the missions' archives, of their sky coverage, number of field observed, and mean, median and total exposures for each filter. We programmatically queried the Milkuski Archive for Space Telescopes (MAST) Portal, requesting positions and exposure times for all observations taken in a given UV filter/instrument/mission combination, and then computed the median, average and total integration time. We also computed the total number of non-repeated fields within a healpix representation whose angular size was approximately one third of the FOV of each instrument, so that fields separated by less than a third of the FOV

counted as a single field. Changes in the metadata account for the differences between the 2020 values presented in the original IAU report and the current Table 1.

The properties of the filters are also summarized with λ_c (the pivot wavelength, as a measure of the central wavelength of a filter (see <https://hst-docs.stsci.edu/wfc3ihb> and [47]), is calculated considering the integrated system throughput), and their full-width at half maximum, $\Delta\lambda$. The sky coverage and fields are displayed in Fig. 2 for some representative surveys, as extracted from an analysis of the metadata of their archives.

Not surprisingly, GALEX, the UV photometric surveyor, has provided the bulk of the information on the UV sky however, as shown in Fig. 2, the vast majority of the data concerning sources located within $\pm 10^\circ$ of the galactic plane has been obtained by the spectroscopic missions and by SWIFT.

Another relevant issue is that there are no photometric measurements below 115 nm. This lower wavelength limit is set by the reflective cut-off of the MgF₂ material used for protective mirror coatings as well as for the sealing / protective window of the MCP detectors operating at wavelengths below 170 nm. There are MCP devices that operate “open faced” and do not suffer this limit, and extend down to 100 nm or lower, but whose response is generally curtailed above 200 nm (they are solar blind).

UV photometry is based on the fluxes measured by the TD1 satellite [46]; magnitudes and standard errors were derived from absolute fluxes by means of the calibration by [27]. Fluxes were measured in four bands with an effective width of ~ 33 nm and centred at 156.5 nm, 196.5 nm, 236.5 nm, and 274.0 nm; however none reaches below 140 nm. As shown in Fig. 1, these bands have not been used much in later missions and, in practice, the spectrophotometric standards in the HST system are now the baseline for flux calibration at UV wavelengths.

The original spectrophotometric standards were defined by the IUE. They were incorporated later into the HST [10]; the 23 original calibration stars and their finding charts can be found in [48]. The conversion of the IUE spectra on the white dwarf primary spectrophotometric scale [11] is described by [8, 9].

The spectrophotometric standards can be accessed through CALSPEC²; only 46 of them have been observed in the full 115–400 nm spectral range and just 3 (including Vega) have been observed with FUSE (i.e. below 115 nm). Most of the sources are either A-type stars or white dwarf stars. Their main characteristics and spatial distribution on the sky are represented in Fig. 3.

In summary, there is no standard system concerning UV photometry. The most frequently available bands are the FUV band (about 140–180 nm) and the NUV band (about 190–250 nm), plus the u-band from the Strömgren photometric system (which is used to bridge the gap to the optical band). Very often, and especially at wavelengths below 200 nm, band selection is not implemented through the use of specific filters, since their construction has been very difficult to achieve. The absolute flux and cross

² <https://www.stsci.edu/hst/instrumentation/reference-data-for-calibration-and-tools/astronomical-catalogs/calspec>

Table 1 UV fields observed before May 2020

Filter	λ_c (nm)	$\Delta\lambda$ (nm)	No. fields	Sky cov. (deg ²)	Mean exp. (s)	Median exp. (s)	Total exp. ² (s)
GALEX							
FUV	152.8	44.2	34199	33264	631	185	21,710,348
NUV	227.1	106.0	44475	39623	898	207	40,230,387
SWIFT/UVOT							
UVW2	203	68.7	41823	3357	1092	536	54,014,523
UVM2	223.1	49.8	46386	3724	1034	529	54,686,775
UVW1	263.4	69.3	47819	3724	845	299.6	48,449,202
ASTROSAT/UVIT							
FUV_F148W	148	50.0	1123	192.1	8599	5000	7,188,450
FUV_F148Wa	148	50.0	1123	192.1	3476	3000	128,599
FUV_F154W	154	38.0	1123	192.1	11307	5000	6,965,232
FUV_F169M	169	29.0	1123	192.1	5058	2924	2,266,156
FUV_F172M	172	12.5	1123	192.1	4603	2000	2,306,158
NUV_N219M	219	27.0	1123	192.1	7022	3496	891,816
NUV_N242W	242	78.5	1123	192.1	7326	3000	923,104
NUV_N245M	245	28.0	1123	192.1	5456	2978	987,560
NUV_N263M	263	27.5	1123	192.1	4256	2100	668,119
NUV_N279N	279	9.0	1123	192.1	5494	3364	901,015

Table 1 continued

Filter	λ_c (nm)	$\Delta\lambda$ (nm)	No. fields	Sky cov. (deg ²)	Mean exp. (s)	Median exp. (s)	Total exp. ² (s)
XMM-NEWTON/OM							
UVW2	212	50	2228	10.52	2668	2499	44,055,184
UVM2	231	48	4074	19.23	2980	3000	70,732,649
UVW1	291	83	5251	24.79	2730	2500	95,506,682
HST/WFPC2							
F160BW	149.2	50.0	737	19.5	642	500	980,225
F170BW	166.6	43.4	976	13.1	381	40	1,441,338
F185W	189.9	29.7	316	4.23	626	300	372,636
F255W	254.5	40.8	1566	20.98	563	200	1,745,273
F300W	289.2	72.8	9356	125.37	1125	800	27,158,110
F336W/	331.7	37.1	7373	202.9	1213	620	23,851,500
Strömgren u							
HST/WFPC3							
F200LP	488.3	50.2	732	9.81	832	600	1,748,562
F218W	222.4	32.2	1238	16.59	566	89	2,423,890
F225W	235.9	46.7	1475	19.76	1162	588	5,993,141
F275W	270.4	39.8	4154	55.66	1623	1010	21,107,717

Table 1 continued

Filter	λ_c (nm)	$\Delta\lambda$ (nm)	No. fields	Sky cov. (deg ²)	Mean exp. (s)	Median exp. (s)	Total exp. ² (s)
HST/ACS, SOLAR BLIND CHANNEL							
F115LP	MgF2 115 nm LP	N/A	384	5.14	274	100	738,466
F122M	142 nm	10	171	2.29	650	160	346,330
F125LP	CaF2 125 nm LP	N/A	501	6.71	402	100	1,256,812
F140LP	BaF2 140 nm LP	N/A	539	7.22	840	100	1,820,292
F150LP	Quartz 150 nm LP	N/A	666	8.92	2500	1840	3,636,616
F165LP	Fused Silica 165 nm LP	N/A	297	3.98	1093	540	782,253
HST/ACS, HIGH RESOLUTION CAMERA							
F220W	222.8	48.5	368	4.93	1624	868	1,346,271
F250W	269.6	54.9	762	10.21	1859	1496	2,467,353
F330W	335.4	58.8	538	7.21	760	300	1,024,954

[1] Data for UVIT are from [45]

[2] Total exposure time obtained by co-adding the individual exposures provided by the archives of the missions

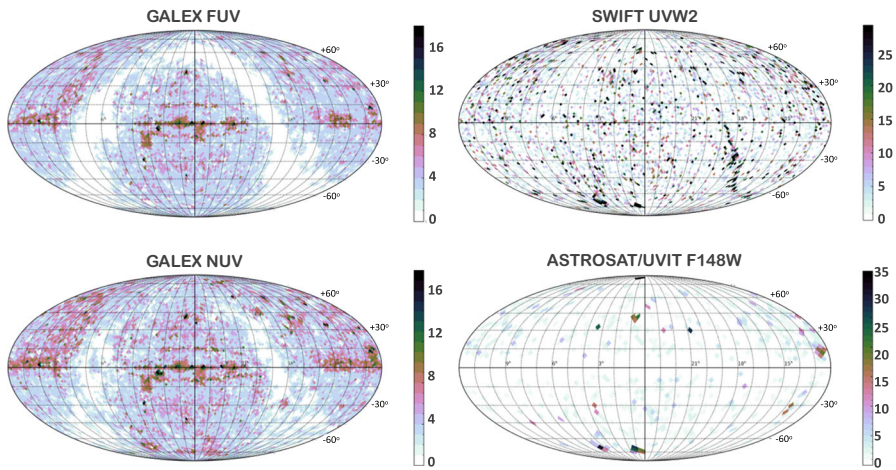


Fig. 2 Sky coverage of the observations made with Astrosat/UVIT/FUV_F148W, SWIFT/UVOT/UVW2, GALEX/FUV and GALEX/NUV. The total number of exposures in a given region is indicated by the color code

talk calibration between missions and instruments is based on the well defined set of spectrophotometric standards maintained by the Hubble Space Telescope.

3 Foreseen characteristics of a UV photometric system suitable for small, cubesat-like missions

In this section, the main technological, environmental and astronomical issues taken into account for the definition of the UV photometric system are summarized. They will affect the definition of new missions when combined with cost-efficiency related issues.

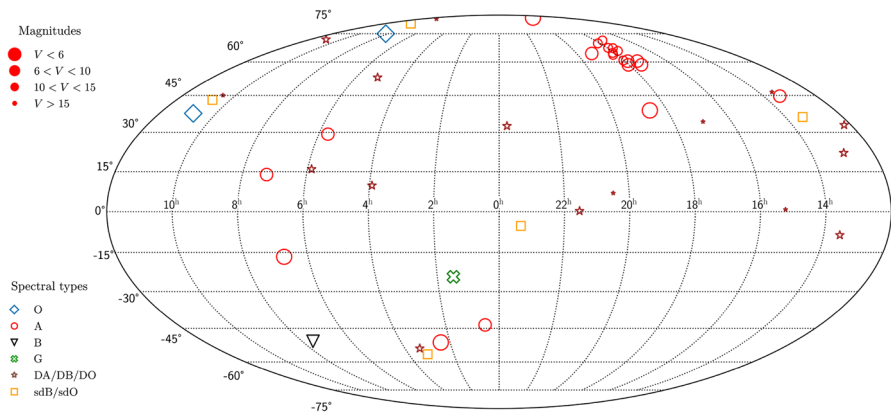


Fig. 3 Distribution of UV photometric standards in the sky

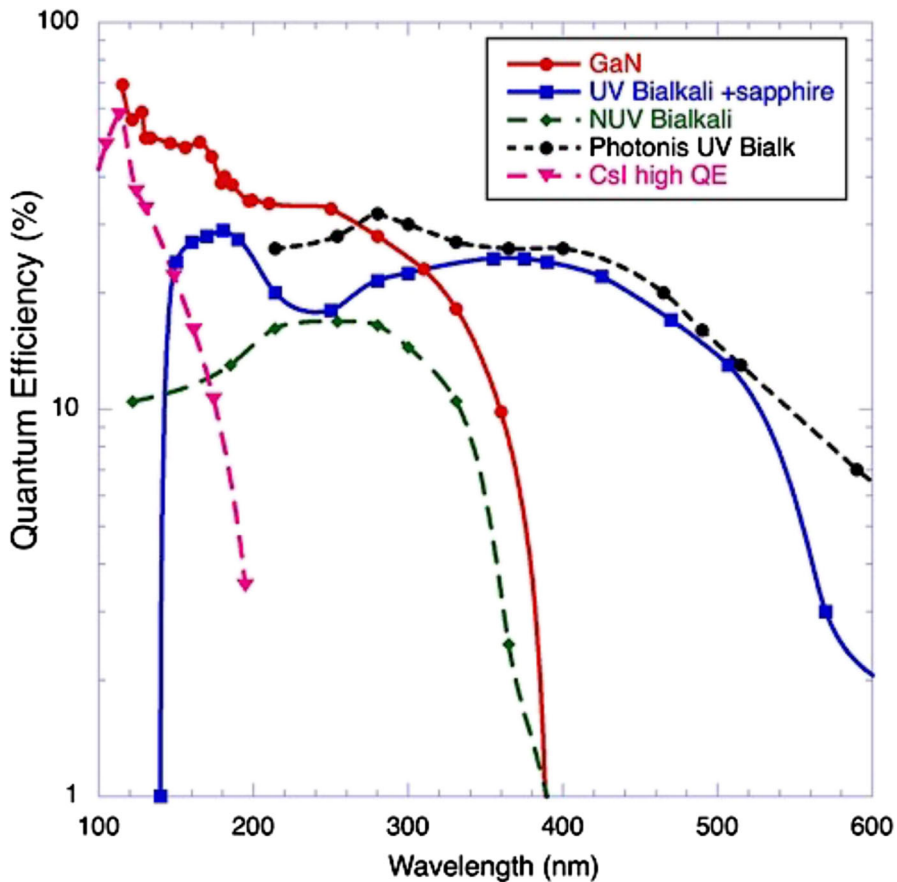


Fig. 4 Summary of photocathode quantum efficiency (QE, %) for opaque and semitransparent UV photocathodes. Comparison for an opaque CsI on a MCP, an opaque GaN on a sapphire substrate, a cutoff tailored NUV semitransparent bialkali on a MgF₂ window, a typical Photonis high QE UV semitransparent bialkali on a fused silica window, and a semitransparent UV bialkali on a sapphire window in a Photonis Planacon MCP detector (https://www.photonis.com/system/files/2020-01/Leaflet_Quantum_Efficiency_Phocadec.pdf). The percentage of ejected photoelectrons per impinging photons is represented in the Y-axis. Semitransparent photocathodes have been used in astronomical applications with efficiencies below 20% in the past. This technology has evolved significantly in the last decade. Depositing the photosensitive substrate directly in the MCP micro-tubes and slight variations in the micro-tubes geometry have proven to increase the efficiency by at least a factor of ~ 2

3.1 Detector and coating technology set the main instrumentation-related constraints

There are two widespread detector technologies used in UV astronomy: micro-channel plates (MCPs) and doped charge coupled devices (CCDs), and one emergent technology: complementary metal oxide semiconductor (CMOS). MCPs are photon counting devices based on a photocathode coupled to a micro-channel plate (MCP) that amplifies the electronic signal generating a shower of typically $\sim 10^5 - 10^6$ secondary

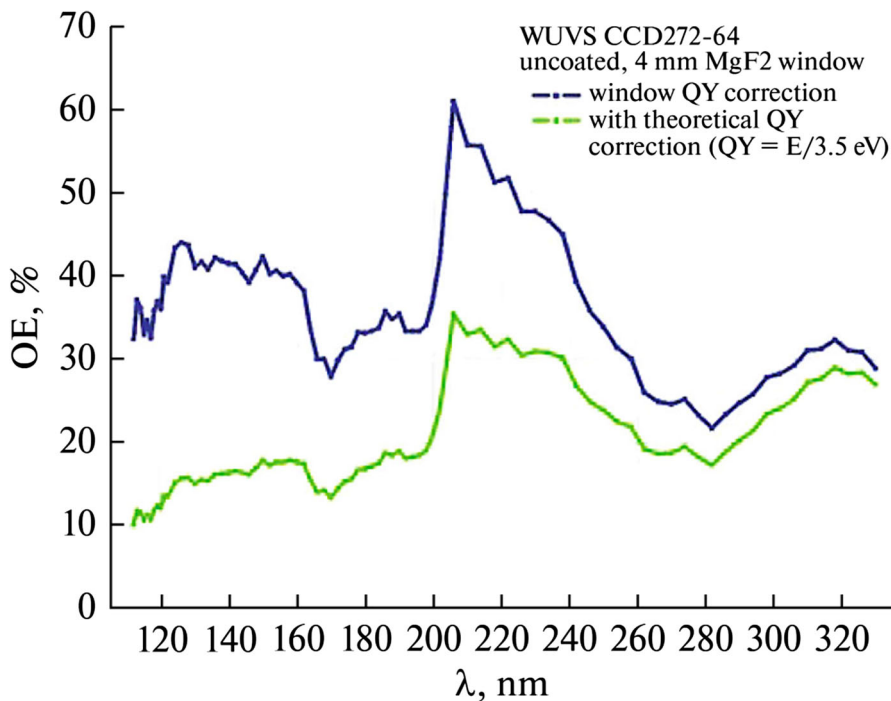


Fig. 5 Quantum yield of the CCD without antireflection coating (blue) and with a correction for the quantum yield effect (green) after [43]

electrons per photoelectron. This electron shower may be read directly using typically wedge- or cross-strip anodes, or transformed into optical photons and then read with conventional optically-coupled CMOS or CCD detectors. MCPs provide fast photon counting (≤ 10 milliseconds) and a well-defined spectral coverage determined by the photocathode material (often CsI or CsTe) and very good out-of-band rejection. In spite of their limitations (small dynamical range and limited lifetime), they have been implemented in most of the UV missions/instruments: GALEX, XMM-Newton/OM, SWIFT/UVOT, HST/ACS, HST/COS, Astrosat/UVIT. Their quantum efficiency is being improved by the use of materials such as GaN or new bi-alkali materials, or by the direct deposition of the photosensitive substrate on the MCP front face (see Fig. 4).

CCDs have flatter efficiencies over the UV range (see Fig. 5) and do not have a limited lifetime however, they are more sensitive in the visible than in the UV range. This becomes a problem, the so-called *red-leak*, when CCDs are used for UV photometric observation of bright optical sources. CCDs for UV astronomy require low working temperatures (140–170K) and are being used in spectroscopic missions such as WSO-UV [43] or CUTE [18].

The newly emergent detector architecture is that of CMOS devices. The only confirmed UV flight mission they have been baselined on at this time is the ULTRASAT

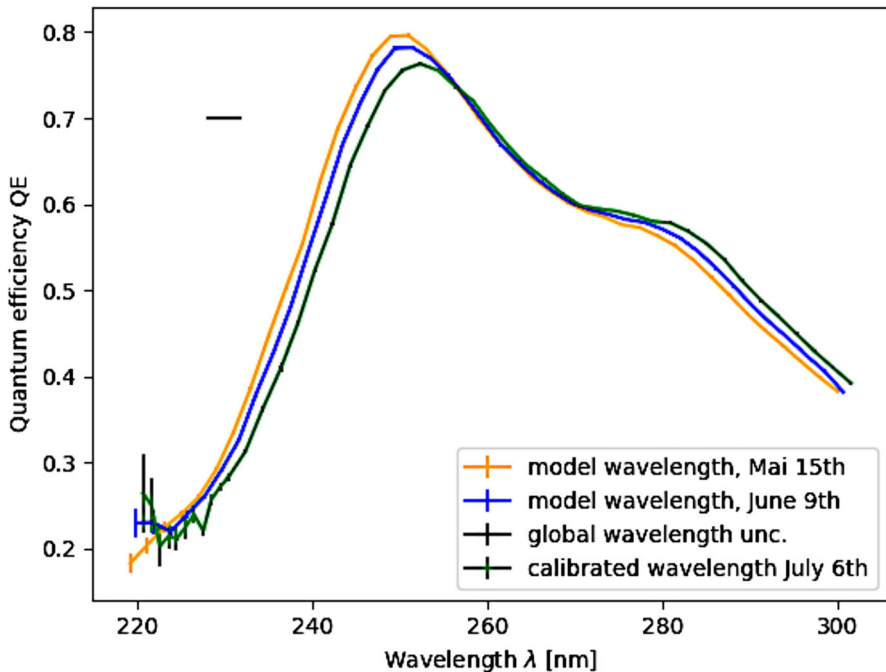


Fig. 6 Shown are three QE scans of the same ULTRASAT test sensor. The measurements are performed in the wavelength range 220–300 nm and over a period of 3 months. The first two measurements are subject to large wavelength uncertainties shown by a black errorbar in the upper left. The last measurement is calibrated using a Holmium Didymium absorption line filter leading to 0.2 nm uncertainties on the measurement [5]

mission to fly in 2025, although they are being considered for the UVEX NASA MIDEX mission currently under study [31]. The devices employ pixels in a 5T-design, that offers dual gain capability enabling a high-dynamic range operation mode. When combined with other standard features for the CMOS architecture such as non-destructive reads, up-the-ramp sampling and the ability to window areas of the device, the number of observing modes is increased dramatically. Like CCDs the devices suffer from a sensitive dependence of dark current on operational temperatures, but unlike CCDs there is no charge transfer efficiency problem – typical operational temperatures are 200K. CMOS devices can also be doped to target specific passbands, as is illustrated in Fig. 6 for the ULTRASAT devices.

FUV filters are challenging to build, their transmittance is typically low (peak transmittance is below 20% for 10 nm passbands) and reaching out-of-band rejections below $\sim 10^{-4}$ is not easy. Early in the 70's, peak transmissions of $\sim 15\%$ were achieved for a 9 nm passband filter at $\text{Ly}\alpha$ using Al/MgF₂ layers deposition on a LiF substrate [33, 34]. These values have not been improved significantly over the intervening years mainly because of the technical difficulties imposed by the micro-roughness of the MgF₂ films, which propagate to the thin Aluminium films causing an increase in the absorption. These older FUV filters also exhibit some performance

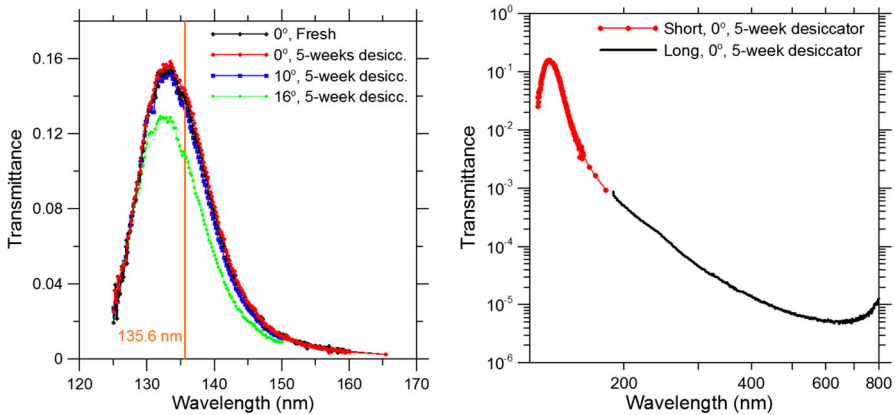


Fig. 7 FUV filters implemented in the Ionosphere Photometer of the Feng Yun-3D meteorological satellite. *Left*: Transmittance as a function of wavelength for a filter peaked at 135.6 nm both fresh (with a short exposure to the atmosphere) and after storage of 5 weeks in a desiccator. Transmittance of the aged sample at 10° and 16° is also displayed. *Right*: Transmittance in logarithmic scale (after [37])

evolution over time as shown in Fig. 7 [37]. More recently, use of techniques such as atomic layer deposition (ALD) [28, 40] have improved the optical uniformity and layer deposition thickness control to offer the possibility of a new generation of FUV interference filters.

A different approach is followed in the filter set implemented in the instrument Advanced CameraSystem (ACS) on HST, where many step filters are implemented in the 115–175 nm range. This enables broad band (bandwidth 30–50 nm) imaging by combining the transmission of a suite of step filters with the spectral sensitivity of the detector; it is, however, affected by red-leak problems.

Most FUV mirrors and gratings are coated with a thin film of MgF_2 to prevent oxidation, but which also sets an effective sensitivity cut-off below 115 nm, which is especially dramatic when MCP detectors using MgF_2 sealing windows are used. This fact has traditionally limited the UV range to above 115 nm (roughly above/below $\text{Ly}\alpha$) and although new technologies may enable the use of LiF to extend access below 115 nm, most existing off the shelf UV reflective surfaces, especially those to be implemented in low cost missions, resort to using MgF_2 for coating and sealing.

3.2 Environmental constraints

Another set of constraints to be considered is the sky background and the in-orbit environmental conditions; the UV background below 180 nm is roughly 4 orders of magnitude weaker than at optical wavelengths, however the upper layers of the Earth's atmosphere produce a few, but very strong, emission lines of oxygen and hydrogen that can severely pollute UV spectra (see Fig. 8). However, astronomical observations from high earth orbit (HEO) satellites are not significantly affected by these lines unless the observing line of sight gets too close to the Earth limb. Observations from

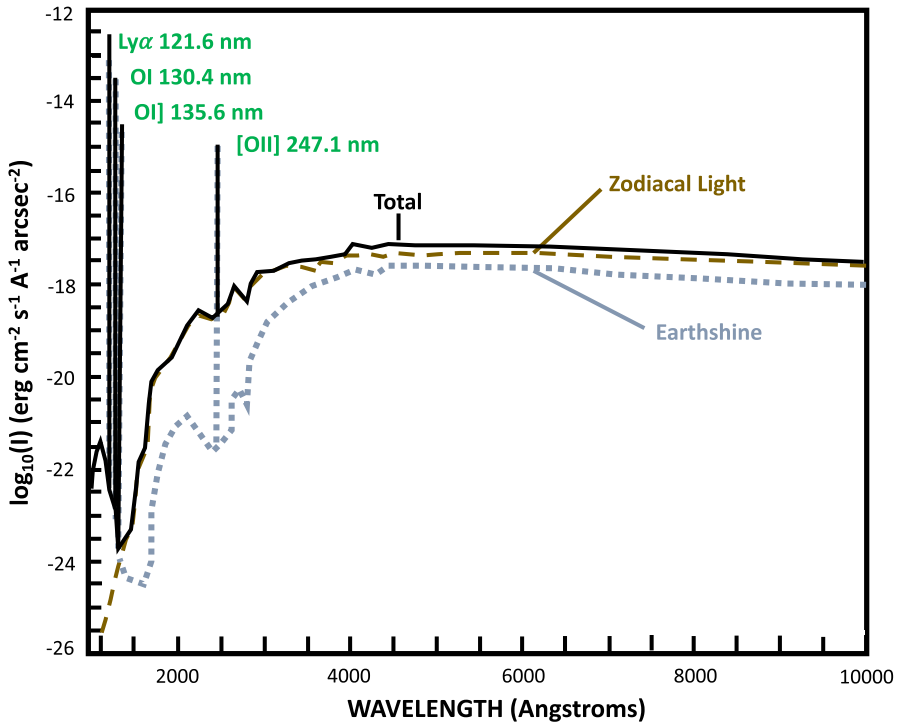


Fig. 8 Sky background intensity. The zodiacal contribution corresponds to $m_V = 22.1 \text{ arcsec}^{-2}$. The earthshine is for a target which is 38° from the limb of the sunlit Earth. The geocoronal airglow line intensities are plotted at “average” intensities (<https://hst-docs.stsci.edu/stisihb/chapter-6-exposure-time-calculations/6-5-detector-and-sky-backgrounds>)

low earth orbit (LEO) satellites can be severely affected, in particular by the Lyman- α transition of hydrogen at 122 nm and the OI triplet resonance transitions at 130.217, 130.486, and 130.603 nm.

3.3 Interstellar extinction

The shape of the interstellar extinction curve can be modelled by a set of polynomial fits that extend from the far UV to the infrared using as free parameter $R_V = A_V/E(B - V)$ [20]. The curve allows a simple parametrization in the infrared that extends smoothly into the optical range and is broken in the UV range by the presence of a strong absorption band (the so-called UV bump) at 225 nm (see Fig. 9). Five coefficients are used for the mathematical representation of the extinction law in the UV which is parametrized as,

$$k(\lambda - V) = E(\lambda - V)/E(B - V) = c_1 + c_2x + c_3D(x, x_0, \gamma) \tag{1}$$

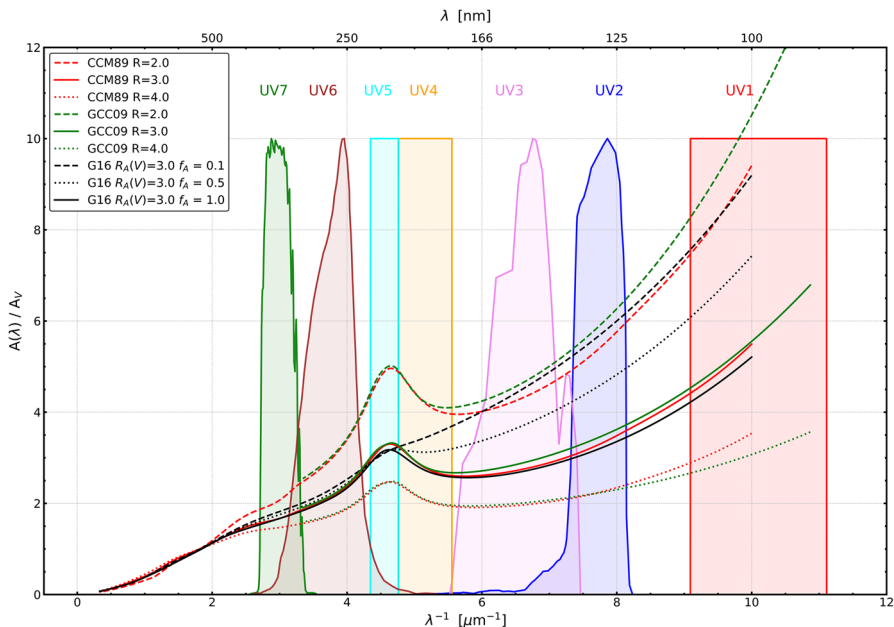


Fig. 9 A sample of extinction curves based on the models CCM89 [12], GCC09 [24] and G16 [25], with variable R_V and mixture parameter f_A . The filter set described in Section 4 fully samples the variability of the extinction curve in a wide variety of environments

with $x = 1/\lambda(\mu\text{m})$ and,

$$D(x, x_0, \gamma) = \frac{x^2}{(x^2 - x_0^2)^2 + x^2\gamma^2} \tag{2}$$

Parameters c_1, c_2, c_3, x_0 and γ are constants that depend on the specific line of sight. The area of the bump is given by $A_{\text{bump}} = \pi c_3 / (2\gamma)$ and its maximum intensity by $I_{\text{bump}} = c_3 / \gamma^2$. The width of the bump varies considerably with the line of sight but its central wavelength remains stable [19]. Originally, it was thought that the bump was produced by small graphite particles however, variations in the graphite grain shape and size should produce variations also in the central wavelength, x_0 [17]. Nowadays, polycyclic-aromatic-hydrocarbons (PAHs) are thought to be the dominant component (see the review by [16] for more details).

The GALEX filter set was defined to compensate for the average galactic extinction. However, some small missions are now being specifically designed to study the distribution and properties of the interstellar dust in the Galaxy, rather than avoid it.

3.4 Other considerations

The density of spectral lines increases rapidly with photon energy, however any attempt to define the photometric system based on binning the UV range into 3-5 energy bins

does not do a good job of reproducing the near UV continuum, and therefore hampers the definition of bands that can be used for the study of the UV extinction bump.

Finally, since GALEX has provided the most extensive survey of the sky at UV wavelengths, it is a desirable feature of any new photometric system that the GALEX FUV and NUV bands should be included. In addition, extending the system up to the atmospheric cut-off at 350 nm is also highly desirable.

4 The photometric system

Based on the criteria exposed in Section 3, the UVA WG proposed a photometric system that consisted of three NUV bands NUV1 (GALEX NUV blue edge to 210 nm), NUV2 (210 nm - 235 nm), and NUV3 (235 nm - 275 nm); the GALEX FUV band; and an additional set of two to three bands to be later defined after consultation with the UV community, which would cover the 90–140 nm spectral range. Feedback from the community was then solicited. A questionnaire was distributed through the International Astronomical Union network, via the website pages belonging to the UVA-WG. Also, a general mailing to the registered members of the global Network for Ultraviolet Astronomy (gnuva.net) was issued; the feedback from this poll is summarized in [Appendix](#). The results from the poll, together with the deliberations of the UVA-WG, were used to define the proposed list of filters that are summarized in [Table 2](#).

To visualize the characteristics of the system, the proposed UV1–UV7 magnitudes have been computed for the Hubble spectrophotometric standards; the UV bands are plotted in [Fig. 10](#) and color-color diagrams for these 45 sources are displayed in [Fig. 11](#).

5 Example of implementation for Smallsats and Cubesats

The Star-Planet Activity Research Cubesat (SPARCS, [1]) is one of a few CubeSats currently under development for astronomical imaging in the ultraviolet. The key scientific objective of the mission is to monitor the high-energy radiation environment of the habitable zone exoplanets around M Dwarfs. Earth-like planets are easier to find around low mass stars and the scientific community is investing significant efforts to detect them. However, unlike solar-type stars, M dwarfs stay active with high emission levels and frequent flares throughout their lives [42]. The effects of sustained high levels of stellar activity on planetary atmospheres have not been studied since UV flare rates and energies across time are not well-known. Yet, we can expect that the increased UV emission and associated particle flux will have dramatic effects on a planet's atmosphere (e.g., [32, 41]). The UV emission probed by SPARCS can, for instance, photodissociate important diagnostic molecules in a planetary atmosphere, such as water (H₂O), ozone (O₃), sulfur dioxide (SO₂, a signature of volcanic activity), and ammonia (NH₃, an important source of the nitrogen required to build amino acids) ([Fig. 12](#), lower panel).

Table 2 UV photometric bands proposed as standards

Band ID	Sp. range	Objective	Comments on implementation
UV1	90–110 nm	FUSE window	[CsI photocathode + F125LP (CaF ₂)] -
UV2	120–140 nm	far UV avoiding geocoronal Ly- α	[CsI photocathode + F140LP (BaF ₂)] As in GALEX
UV3	140–180 nm	GALEX FUV	
UV4	180–210 nm	Continuum shortward of the UV bump	
UV5	210–230 nm	UV bump	
UV6	230–280 nm	Near UV continuum, Fe bands	F250W (ACS/HRC)
UV7	280–350 nm	Ozone cut-off window	F330W (ACS/HRC)

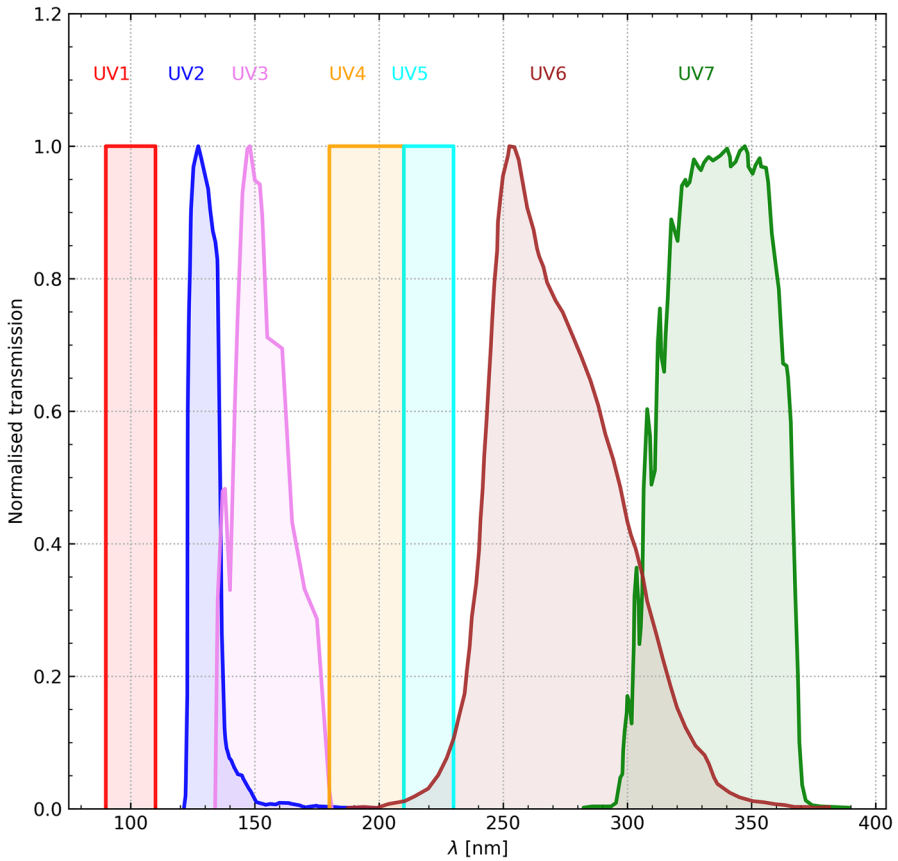


Fig. 10 The IAU-recommended UV bands. Some of them, UV2, UV3, UV6 and UV7, are already in use since they come from the Hubble instruments or from GALEX. For the new bands, simple (unrealistic) boxcar functions have been used with transmittances similar to the rest of the bands. See Table 2 for a summary

The transmittance of the filters (including the contribution from the detector spectral sensitivity) is shown in Fig. 13. The filter S-FUV is slightly shifted with respect to UV3 (GALEX FUV) to optimize the sensitivity to the CIV and He II lines. The filter S-NUV is similar to UV6 and the S-MUV is the sum of filters UV4+UV5.

SPARCS bands were defined for a very specific scientific purpose, and yet they are very close to the UV1-UV7 system proposed in this report. Moreover, given that the underlying spectral energy distribution of the sources is known (M-type stars), SPARCS magnitudes could easily be converted into the standard UV1-UV7 photometric system.

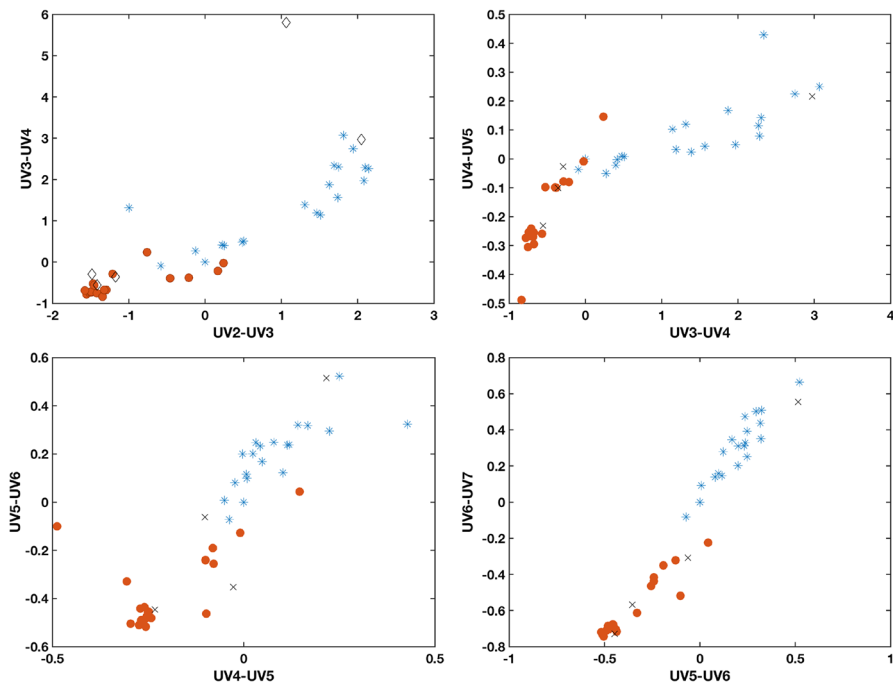


Fig. 11 Color-color diagrams for the UV spectrophotometric standards (red circles: white dwarfs; asterisks: A-type stars; black crosses: other types)

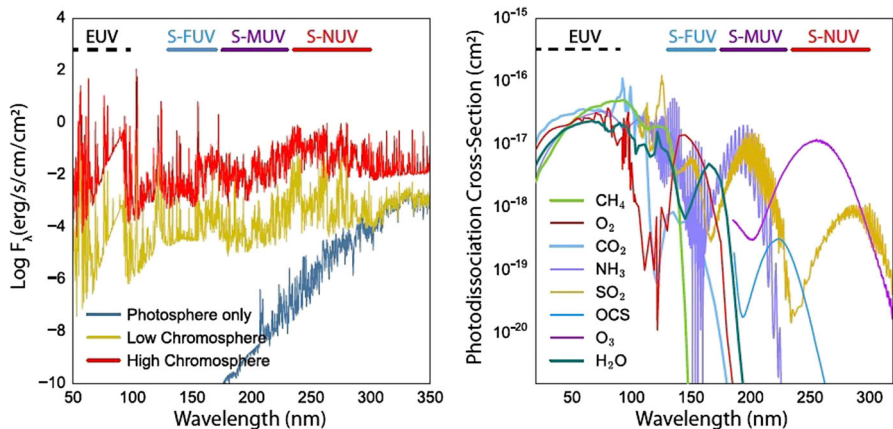


Fig. 12 SPARCS UV filters probe key spectral regions important for both M dwarf non-thermal emission and exoplanet atmospheric molecules. Top: UV emission from M dwarfs atmosphere. Bottom: Cross section to photodissociation by UV radiation of relevant atmospheric molecules. The spectral coverage of the SPARCS UV filters (S-FUV, S-MUV, S-NUV) is shown in both panels

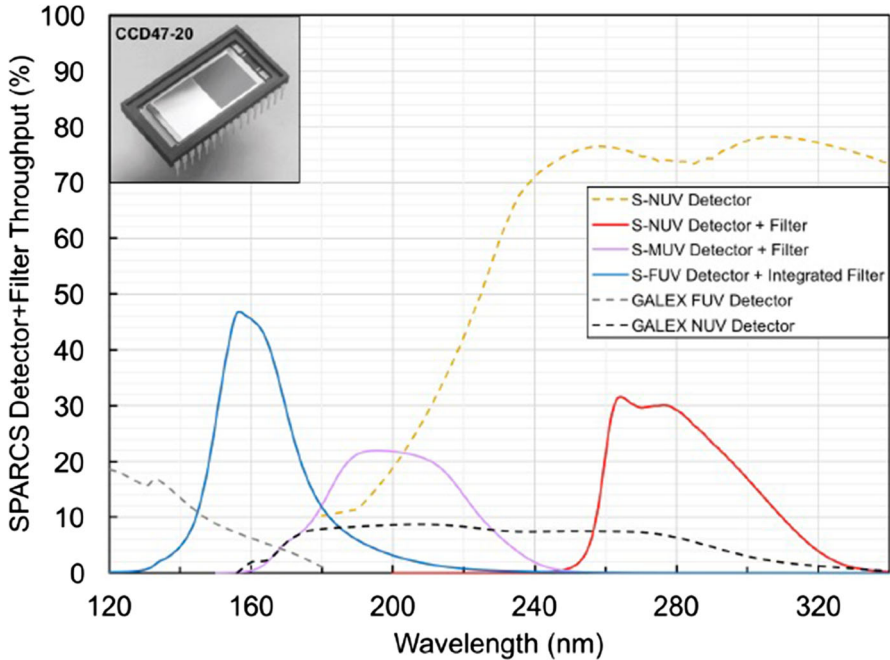


Fig. 13 SPARCS throughput in the S-FUV, S-MUV and S-NUV bands

6 Summary and conclusions

Along with an overview of the astronomical instrumentation used to carry out UV photometry, this article presents the standard photometric system for UV astronomy approved by the IAU during the General Assembly in 2021, that should to be regarded as a tool for homogenizing photometry as part of the post-processing of the data. Its implementation is feasible because many missions and researchers have independently defined filters for their science that are rather similar (see Fig. 1), so translating them into the IAU standard system is straightforward. The implementation of such a system is crucial for the efficient and transparent use of the large wealth of data that is likely to be acquired in the near future.

The photometric system proposed in Section 4 cannot be implemented in terms of the optical description (transmission curves) of filters. The reflectivity of the coatings and the sensitivity of the detectors vary significantly across the UV spectral range; as shown in Fig. 13, the performance of a UV instrument depends on the combined contributions of all these components. As a consequence, the implementation of the system needs to be done “a posteriori” by post-processing the data from the individual missions into the standard system. The methods to define this standardization constitute the current core of the activity of the UVA WG. The computational resources are already available and the wealth of information in the astronomical archives will certainly aid in this process.

This type of activity fulfills one of IAU's fundamental roles: to define standards of reference for information exchange. The fundamentals of the scientific method require the ability to test results by independent researchers which requires the definition of a clear and accessible framework for the interpretation of the data.

Finally, we would like to emphasize that there are currently several UV missions in definition, each with a different set of filters, and it would be very convenient to have a common framework for broad band photometry in all of the them.

Acknowledgements The authors are grateful to the persons listed in the Appendix for their suggestions, and thank Prof. Jayant Murthy, Prof. Swarna K. Ghosh and the UVIT team for their kind help providing key metadata of the UVIT archive. Some of the data presented in this paper were obtained from the Mikulski Archive for Space Telescopes (MAST). STScI is operated by the Association of Universities for Research in Astronomy, Inc., under NASA contract NAS5-26555. Support for MAST for non-HST data is provided by the NASA Office of Space Science via grant NNX13AC07G and by other grants and contracts. This research made use of `astropy`, a community-developed core Python package for Astronomy [3, 4] and `matplotlib`, a Python library for publication quality graphics [29].

Author Contributions This article contains the report produced by the Working Group (WG) on Ultraviolet Astronomy of the International Astronomical Union (IAU) which set the baseline for the definition of standard bands in UV photometry for Astronomy and it is recommended by the IAU (Recommendation approved in the General Assembly held in 2021). The WG was constituted by all the authors in this article. The report was written by Prof. Ana I Gómez de Castro, chair of the WG. The detailed statistical analysis of the contents of the UV data bases (and the associated figures) was made by Prof. Ana I Gómez de Castro, Dr. David Valls-Gabaud, Dr. Daniela Bettoni and Dr. Leire Beitia-Antero. Dr Paul A. Scowen provided the information on the mission SPARCS and contributed to the text in Sections 3 and 5. The text was revised by all the authors.

Funding Open Access funding provided thanks to the CRUE-CSIC agreement with Springer Nature.

Open Access This article is licensed under a Creative Commons Attribution 4.0 International License, which permits use, sharing, adaptation, distribution and reproduction in any medium or format, as long as you give appropriate credit to the original author(s) and the source, provide a link to the Creative Commons licence, and indicate if changes were made. The images or other third party material in this article are included in the article's Creative Commons licence, unless indicated otherwise in a credit line to the material. If material is not included in the article's Creative Commons licence and your intended use is not permitted by statutory regulation or exceeds the permitted use, you will need to obtain permission directly from the copyright holder. To view a copy of this licence, visit <http://creativecommons.org/licenses/by/4.0/>.

Appendix: Poll results

In May 2019, a questionnaire was distributed to astronomers world-wide with the following language:

The current aim of the IAU WG on UV astronomy is to define a standard photometric system for the 900-3000 Angstroms spectral range. The initially proposed photometric system is composed of:

- Three NUV bands: NUV1(GALEX NUV blue edge to 210 nm), NUV2 (210 nm - 235 nm), NUV3 (235 nm - 275 nm).
- the GALEX FUV band.
- Two to three additional bands (to be defined) to cover the 90-140nm spectral range.

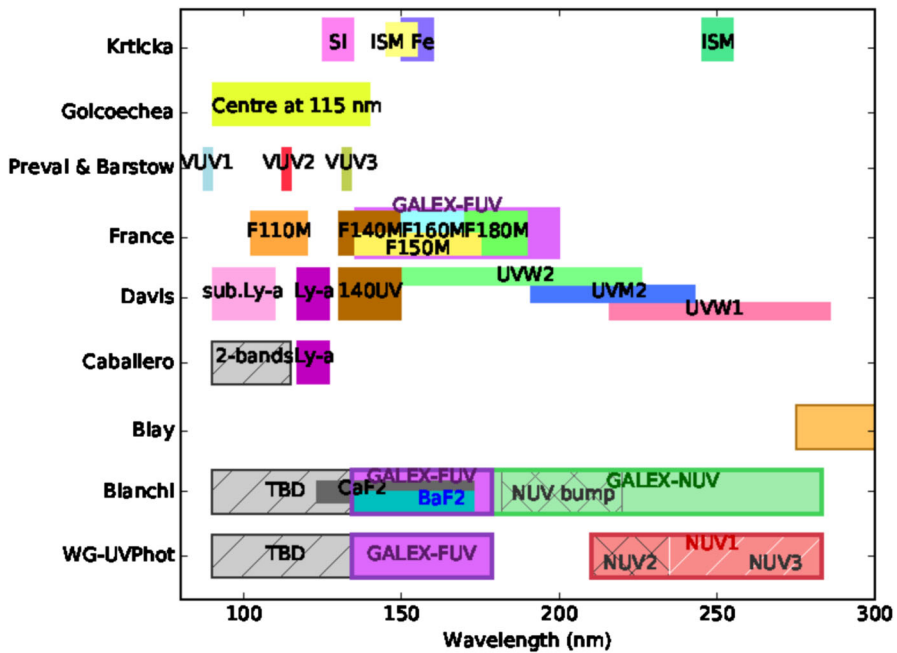


Fig. 14 Summary of the bands proposed by the community in response to the questionnaire

We solicit comments on the above proposed photometric system, or suggestions about alternative filters that could be useful for future UV science. Ideally, the proposed filters should be versatile and practical for different astrophysical studies. The deadline to send your proposals is June 7th.

The IAU WG on UV Astronomy

The responses to the Poll are summarized in Fig. 14 where the range of alternative filter sets proposed by the members of the community are plotted and compared with the original set proposed by the UVA-WG.

References

1. Ardila, D.R., Shkolnik, E., Scowen, P., et al.: The Star-Planet Activity Research CubeSat (SPARCS): A Mission to Understand the Impact of Stars in Exoplanets. (2018). [arXiv:1808.09954](https://arxiv.org/abs/1808.09954) [astro-ph.IM]
2. Ardila, D. R., Shkolnik, E., Ziemer, J., et al.: The UV-SCOPE mission: ultraviolet spectroscopic characterization of planets and their environments. In: den Herder, J. W. A., Nikzad, S., Nakazawa, K. (eds) Space Telescopes and Instrumentation 2022: Ultraviolet to Gamma Ray, pp. 1218104. (2022). <https://doi.org/10.1117/12.2629000>, 2208.09547
3. Astropy Collaboration, Robitaille, T.P., Tollerud, E.J., Greenfield, P., Droettboom, M., Bray, E., Aldcroft, T., Davis, M., Ginsburg, A., Price-Whelan, A.M., Kerzendorf, W.E., Conley, A., Crighton, N., Barbary, K., Muna, D., Ferguson, H., Grollier, F., Parikh, M.M., Nair, P.H., Unther, H.M., Deil, C., Woillez, J., Conseil, S., Kramer, R., Turner, J.E.H., Singer, L., Fox, R., Weaver, B.A., Zabalza, V., Edwards, Z.I., Azalee Bostroem, K., Burke, D.J., Casey, A.R., Crawford, S.M., Dencheva, N., Ely, J., Jenness, T., Labrie, K., Lim, P.L., Pierfederici, F., Pontzen, A., Ptak, A., Refsdal, B., Servillat, M.,

- Streicher, O.: Astropy: A community Python package for astronomy. *Astron. Astrophys.* **558**, A33 (2013). <https://doi.org/10.1051/0004-6361/201322068>
4. Astropy Collaboration, Price-Whelan, A.M., Sipöcz, B.M., Günther, H.M., Lim, P.L., Crawford, S.M., Conseil, S., Shupe, D.L., Craig, M.W., Dencheva, N., Ginsburg, A., VanderPlas, J.T., Bradley, L.D., Pérez-Suárez, D., de Val-Borro, M., Aldcroft, T.L., Cruz, K.L., Robitaille, T.P., Tollerud, E.J., Ardelean, C., Babej, T., Bach, Y.P., Bache, M., Bakanov, A.V., Bamford, S.P., Barentsen, G., Barmby, P., Baumbach, A., Berry, K.L., Biscani, F., Boquien, M., Bostroem, K.A., Bouma, L.G., Brammer, G.B., Bray, E.M., Breytenbach, H., Buddelmeijer, H., Burke, D.J., Calderone, G., Cano Rodríguez, J.L., Cara, M., Cardoso, J.V.M., Cheedella, S., Copin, Y., Corrales, L., Crichton, D., D'Avella, D., Deil, C., Depagne, É., Dietrich, J.P., Donath, A., Droettboom, M., Earl, N., Erben, T., Fabbro, S., Ferreira, L.A., Finethy, T., Fox, R.T., Garrison, L.H., Gibbons, S.L.J., Goldstein, D.A., Gommers, R., Greco, J.P., Greenfield, P., Groener, A.M., Grollier, F., Hagen, A., Hirst, P., Homeier, D., Horton, A.J., Hosseinzadeh, G., Hu, L., Hunkeler, J.S., Ivezic, Ž., Jain, A., Jenness, T., Kanarek, G., Kendrew, S., Kern, N.S., Kerzendorf, W.E., Khvalko, A., King, J., Kirkby, D., Kulkarni, A.M., Kumar, A., Lee, A., Lenz, D., Littlefair, S.P., Ma, Z., Macleod, D.M., Mastrogiuseppe, M., McCully, C., Montagnac, S., Morris, B.M., Mueller, M., Mumford, S.J., Muna, D., Murphy, N.A., Nelson, S., Nguyen, G.H., Ninan, J.P., Nöthe, M., Ogaz, S., Oh, S., Parejko, J.K., Parley, N., Pascual, S., Patil, R., Patil, A.A., Plunkett, A.L., Prochaska, J.X., Rastogi, T., Reddy Janga, V., Sabater, J., Sakurikar, P., Seifert, M., Sherbert, L.E., Sherwood-Taylor, H., Shih, A.Y., Sick, J., Silbiger, M.T., Singanamalla, S., Singer, L.P., Sladen, P.H., Soolley, K.A., Sornarajah, S., Streicher, O., Teuben, P., Thomas, S.W., Tremblay, G.R., Turner, J.E.H., Terrón, V., van Kerkwijk, M.H., de la Vega, A., Watkins, L.L., Weaver, B.A., Whitmore, J.B., Woillez, J., Zabalza, V., Astropy Contributors: The Astropy Project: Building an Open-science Project and Status of the v2.0 Core Package. *Astron. J.* **156**, 123 (2018). <https://doi.org/10.3847/1538-3881/aabc4f>
 5. Bastian-Querner, B., Kaipachery, N., Küster, D., et al.: Sensor characterization for the ULTRASAT space telescope. In: Barto, A. A., Breckinridge, J. B., Stahl, H. P. (eds) *UV/Optical/IR Space Telescopes and Instruments: Innovative Technologies and Concepts X*, pp. 118190F. (2021). <https://doi.org/10.1117/12.2593897>, 2108.02521
 6. Ben-Ami, S., Shvartzvald, Y., Waxman, E., et al.: The scientific payload of the ultraviolet transient astronomy satellite (ULTRASAT). In: den Herder, J. W. A., Nikzad, S., Nakazawa, K. (eds) *Space Telescopes and Instrumentation 2022: Ultraviolet to Gamma Ray*, pp. 1218105. (2022). <https://doi.org/10.1117/12.2629850>, 2208.00159
 7. Boggess, A., Carr, F.A., Evans, D.C., et al.: The IUE spacecraft and instrumentation. *Nature* **275**(5679), 372–377 (1978). <https://doi.org/10.1038/275372a0>
 8. Bohlin, R.: Preliminary comparison of the HST and white dwarf absolute flux scales. In: Blades, J. C., Osmer, S. J. (eds) *Calibrating Hubble Space Telescope*, pp. 234. (1994)
 9. Bohlin, R.C.: Spectrophotometric standards from the Far-UV to the Near-IR on the white dwarf flux scale. *Astron. J.* **111**, 1743 (1996). <https://doi.org/10.1086/117914>
 10. Bohlin, R. C., Harris, A. W., Holm, A. V., et al.: The ultraviolet calibration of the hubble space telescope. IV. absolute IUE fluxes of hubble space telescope standard stars. *Astrophys. J. Suppl. Ser.* **73**, 413 (1990). <https://doi.org/10.1086/191474>
 11. Bohlin, R.C., Colina, L., Finley, D.S.: White dwarf standard stars: G191–B2B, GD 71, GD 153, HZ 43. *Astron. J.* **110**, 1316 (1995). <https://doi.org/10.1086/117606>
 12. Cardelli, J.A., Clayton, G.C., Mathis, J.S.: The Relationship between Infrared, Optical, and Ultraviolet Extinction. *Astrophys. J.* **345**, 245 (1989). <https://doi.org/10.1086/167900>
 13. Carruthers, G.R., Page, T.: Apollo 16 Far-Ultraviolet Camera/Spectrograph: Earth Observations. *Science* **177**(4051), 788–791 (1972). <https://doi.org/10.1126/science.177.4051.788>
 14. Chung, H., Vargas, C. J., Hamden, E., et al.: Aspera: the UV SmallSat telescope to detect and map the warm-hot gas phase in nearby galaxy halos. In: Barto, A. A., Breckinridge, J. B., Stahl, H. P. (eds) *UV/Optical/IR Space Telescopes and Instruments: Innovative Technologies and Concepts X*, pp. 1181903. (2021). <https://doi.org/10.1117/12.2593001>
 15. Côté, P.: Wide-field UV imaging: Current capabilities and performance requirements for future missions. *Advances in Space Research* **53**(6), 982–989 (2014). <https://doi.org/10.1016/j.asr.2013.11.033>
 16. Draine, B. T.: Interstellar dust grains. *Annu. Rev. Astron. Astrophys.* **41**, 241–289 (2003). <https://doi.org/10.1146/annurev.astro.41.011802.094840>. arXiv:astro-ph/0304489 [astro-ph]
 17. Draine, B.T., Malhotra, S.: On graphite and the 2175 angstrom extinction profile. *Astrophys. J.* **414**, 632 (1993). <https://doi.org/10.1086/173109>

18. Egan, A., Fleming, B. T., France, K., et al.: The Colorado ultraviolet transit experiment (CUTE): final design and projected performance. In: den Herder, J. W. A., Nikzad, S., Nakazawa, K. (eds) *Space Telescopes and Instrumentation 2018: Ultraviolet to Gamma Ray*, pp. 106990C. (2018). <https://doi.org/10.1117/12.2309990>
19. Fitzpatrick, E. L., Massa, D.: An analysis of the shapes of ultraviolet extinction curves. I. The 2175 angstrom bump. *Astrophys. J.* **307**, 286 (1986). <https://doi.org/10.1086/164415>
20. Fitzpatrick, E. L., Massa, D.: An analysis of the shapes of interstellar extinction curves. V. The IR-through-UV curve morphology. *Astrophys. J.* **663**(1), 320–341 (2007). <https://doi.org/10.1086/518158>. [arXiv:0705.0154](https://arxiv.org/abs/0705.0154) [astro-ph]
21. France, K., Fleming, B., Egan, A., et al.: The colorado ultraviolet transit experiment mission overview. *Astron. J.* **165**(2), 63 (2023). <https://doi.org/10.3847/1538-3881/aca8a2>. [arXiv:2301.02250](https://arxiv.org/abs/2301.02250) [astro-ph.IM]
22. Gehrels, N., Chincarini, G., Giommi, P., et al.: The swift gamma-ray burst mission. *Astrophys. J.* **611**(2), 1005–1020 (2004). <https://doi.org/10.1086/422091>, [arXiv:astro-ph/0405233](https://arxiv.org/abs/astro-ph/0405233) [astro-ph]
23. Gómez de Castro, A. I., Barstow, M. A., Brosch, N., et al.: UV facilities for the investigation of the origin of life. In: Gómez de Castro, A. I. (ed) *Ultraviolet Astronomy and the Quest for the Origin of Life*. Elsevier, pp. 115–160. (2021). <https://doi.org/10.1016/B978-0-12-819170-5.00004-X>
24. Gordon, K.D., Cartledge, S., Clayton, G.C.: FUSE Measurements of Far-Ultraviolet Extinction. III. The Dependence on R(V) and Discrete Feature Limits from 75 Galactic Sightlines. *Astrophys. J.* **705**(2), 1320–1335 (2009). <https://doi.org/10.1088/0004-637X/705/2/1320>
25. Gordon, K.D., Foesneau, M., Arab, H., Tchernyshyov, K., Weisz, D.R., Dalcanton, J.J., Williams, B.F., Bell, E.F., Bianchi, L., Boyer, M., Choi, Y., Dolphin, A., Girardi, L., Hogg, D.W., Kalirai, J.S., Kapala, M., Lewis, A.R., Rix, H-W., Sandstrom, K., Skillman, E.D.: The Panchroma+c Hubble Andromeda Treasury. XV. The BEAST: Bayesian Extinction and Stellar Tool. *Astrophys. J.* **826**(2), 104 (2016). <https://doi.org/10.3847/0004-637X/826/2/104>
26. Hamden, E. T., Schiminovich, D., Nikzad, S., et al.: Hyperion: the origin of the stars. A far UV space telescope for high-resolution spectroscopy over wide fields. *Journal of Astronomical Telescopes, Instruments, and Systems* **8**, 044008 (2022). <https://doi.org/10.1117/1.JATIS.8.4.044008>, [arXiv:2212.06869](https://arxiv.org/abs/2212.06869) [astro-ph.SR]
27. Hayes, D.S., Latham, D.W.: A rediscussion of the atmospheric extinction and the absolute spectral-energy distribution of Vega. *Astrophys. J.* **197**, 593–601 (1975). <https://doi.org/10.1086/153548>
28. Hennessy, J., Jewell, A. D., Hoenk, M. E., et al.: Advances in detector-integrated filter coatings for the far ultraviolet. In: Siegmund, O. H. (ed) *UV, X-Ray, and Gamma-Ray Space Instrumentation for Astronomy XXII*, pp. 118211A (2021). <https://doi.org/10.1117/12.2595524>
29. Hunter, J. D.: Matplotlib: A 2D graphics environment. *Comput. Sci. Eng.* **9**(3), 90–95 (2007)
30. Jansen, F., Lumb, D., Altieri, B., et al.: XMM-Newton observatory. I. The spacecraft and operations. *Astron. Astrophys.* **365**, L1–L6 (2001). <https://doi.org/10.1051/0004-6361:20000036>
31. Kulkarni, S. R., Harrison, F. A., Grefenstette, B. W., et al.: Science with the Ultraviolet Explorer (UVEX). (2021). <https://doi.org/10.48550/arXiv.2111.15608>. [arXiv:2111.15608](https://arxiv.org/abs/2111.15608). [astro-ph.GA]
32. Luger, R., Barnes, R.: Extreme water loss and abiotic O₂ buildup on planets throughout the habitable zones of M dwarfs. *Astrobiology* **15**(2), 119–143 (2015). <https://doi.org/10.1089/ast.2014.1231>. [arXiv:1411.7412](https://arxiv.org/abs/1411.7412) [astro-ph.EP]
33. Malherbe, A.: Interference filters for the far ultraviolet. *Appl. Opt.* **13**(6), 1275 (1974). <https://doi.org/10.1364/AO.13.001275>
34. Malherbe, A.: Multidielectric components for the far ultraviolet. *Appl. Opt.* **13**(6), 1276 (1974). <https://doi.org/10.1364/AO.13.001276>
35. Martin, D. C., Fanson, J., Schiminovich, D., et al.: The galaxy evolution explorer: a space ultraviolet survey mission. *Astrophys. J. Lett.* **619**(1), L1–L6 (2005). <https://doi.org/10.1086/426387>. [arXiv:astro-ph/0411302](https://arxiv.org/abs/astro-ph/0411302) [astro-ph]
36. Moos, H. W., Cash, W. C., Cowie, L. L., et al.: Overview of the Far Ultraviolet Spectroscopic Explorer Mission. *Astrophys. J. Lett.* **538**(1), L1–L6 (2000). <https://doi.org/10.1086/312795>. [arXiv:astro-ph/0005529](https://arxiv.org/abs/astro-ph/0005529) [astro-ph]
37. Rodríguez-De Marcos, L., Larraquert, J.I., Méndez, J.A., et al.: Narrowband filters for the FUV range. In: Takahashi, T., den Herder, J. W. A., Bautz, M. (eds) *Space Telescopes and Instrumentation 2014: Ultraviolet to Gamma Ray*, pp. 914437. (2014). <https://doi.org/10.1117/12.2056666>

38. Rogerson, J.B., Spitzer, L., Drake, J.F., et al.: Spectrophotometric results from the copernicus satellite. I. instrumentation and performance. *Astrophys. J. Lett.* **181**, L97–L102 (1973). <https://doi.org/10.1086/181194>
39. Sachkov, M., Gómez de Castro, A.I., Shustov, B.: The World Space Observatory: ultraviolet mission: science program and status report. In: Society of Photo-Optical Instrumentation Engineers (SPIE) Conference Series, pp. 1144473. (2020). <https://doi.org/10.1117/12.2562929>
40. Scowen, P.A., Nemanich, R., Eller, B., et al.: Use of plasma enhanced ALD to construct efficient interference filters for astronomy in the FUV. In: Navarro, R., Burge, J.H. (eds) *Advances in Optical and Mechanical Technologies for Telescopes and Instrumentation II*, pp. 99122F (2016). <https://doi.org/10.1117/12.2232704>
41. Segura, A., Walkowicz, L.M., Meadows, V., et al.: The effect of a strong stellar flare on the atmospheric chemistry of an earth-like planet orbiting an M dwarf. *Astrobiology* **10**(7), 751–771 (2010). <https://doi.org/10.1089/ast.2009.0376>. [arXiv:1006.0022](https://arxiv.org/abs/1006.0022) [astro-ph.EP]
42. Shkolnik, E.L., Barman, T.S.: HAZMAT. I. The Evolution of Far-UV and Near-UV emission from early M stars. *Astron. J.* **148**(4), 64 (2014). <https://doi.org/10.1088/0004-6256/148/4/64>. [arXiv:1407.1344](https://arxiv.org/abs/1407.1344) [astro-ph.SR]
43. Shugarov, A.S., Sachkov, M., Bruce, G., et al.: WSO-UV mission WUVS instrument FUV-UV CCD detectors qualification campaign main results. In: Society of Photo-Optical Instrumentation Engineers (SPIE) Conference Series, pp. 118525D. (2021). <https://doi.org/10.1117/12.2599948>
44. Singh, K.P., Tandon, S.N., Agrawal, P.C., et al.: ASTROSAT mission. In: Takahashi, T., den Herder, J. W. A., Bautz, M. (eds) *Space Telescopes and Instrumentation 2014: Ultraviolet to Gamma Ray*, p 91441S. (2014). <https://doi.org/10.1117/12.2062667>
45. Tandon, S.N., Postma, J., Joseph, P., et al.: Additional calibration of the ultraviolet imaging telescope on board AstroSat. *Astron. J.* **159**(4), 158 (2020). <https://doi.org/10.3847/1538-3881/ab72a3>. [arXiv:2002.01159](https://arxiv.org/abs/2002.01159) [astro-ph.IM]
46. Thompson, G.I., Nandy, K., Jamar, C., et al.: Catalogue of stellar ultraviolet fluxes : a compilation of absolute stellar fluxes measured by the Sky Survey Telescope (S2/68) aboard the ESRO satellite TD-1. Scientific Research Council (1978)
47. Tokunaga, A.T., Vacca, W.D.: The Mauna Kea Observatories Near-Infrared Filter Set. III. Isophotal Wavelengths and Absolute Calibration. *Publ. Astron. Soc. Pac.* **117**(830):421–426 (2005). <https://doi.org/10.1086/429382>. [arXiv:astro-ph/0502120](https://arxiv.org/abs/astro-ph/0502120) [astro-ph]
48. Turnshek, D.A., Bohlin, R.C., Williamson, I.R.L., et al.: An atlas of hubble space telescope photometric, spectrophotometric, and polarimetric calibration objects. *Astron. J.* **99**, 1243 (1990). <https://doi.org/10.1086/115413>
49. Valls-Gabaud, D., MESSIER Collaboration: The MESSIER surveyor: unveiling the ultra-low surface brightness universe. In: Gil de Paz, A., Knapen, J.H., Lee, J.C. (eds) *Formation and Evolution of Galaxy Outskirts*, pp. 199–201, (2017). <https://doi.org/10.1017/S1743921316011388>

Publisher's Note Springer Nature remains neutral with regard to jurisdictional claims in published maps and institutional affiliations.

Authors and Affiliations

Ana I. Gómez de Castro^{1,2} · **Noah Brosch**³ · **Daniela Bettoni**⁴ ·
Leire Beitia-Antero^{1,5} · **Paul Scowen**⁶ · **David Valls-Gabaud**⁷ ·
Mikhail Sachkov⁸

- ¹ Joint Center for Ultraviolet Astronomy, Universidad Complutense de Madrid, Avda Puerta de Hierro s/n, 28040 Madrid, Spain
- ² Sección Departamental, Departamento de Física de la Tierra y Astrofísica, Universidad Complutense de Madrid, Plaza de Ciencias 3, 28040 Madrid, Spain
- ³ The Wise Observatory and the Raymond and Beverly Sackler School of Physics and Astronomy, Tel Aviv University, 669978 Tel Aviv, Israel
- ⁴ INAF-Osservatorio Astronomico di Padova, INAF, Vicolo dell'Osservatorio 5, I-35122 Padova, Italy
- ⁵ Departamento de Estadística e Investigación Operativa, Universidad Complutense de Madrid, Plaza de Ciencias 3, 28040 Madrid, Spain
- ⁶ Code 667, Exoplanets and Stellar Astrophysics Lab, NASA Goddard Space Flight Center, 8800 Greenbelt Road, 20771 Greenbelt, MD, USA
- ⁷ LERMA, CNRS UMR 8112, Observatoire de Paris, 61 Avenue de l'Observatoire, 75014 Paris, France
- ⁸ Institute of Astronomy, Russian Academy of Sciences, Pyatnitskaya str., 48, 119017 Moscow, Russia